

This is the author's manuscript for publication. The publisher-formatted version may be available through the publisher's web site or your institution's library.

## **Torrefaction of Conservation Reserve Program biomass: a techno-economic evaluation**

Feng Xu, Kyle Linnebur, and Donghai Wang

### **How to cite this manuscript**

If you make reference to this version of the manuscript, use the following information:

Xu, F., Linnebur, K., & Wang, D. (2014). Torrefaction of conservation reserve program biomass: A techno-economic evaluation. Retrieved from <http://krex.ksu.edu>

### **Published Version Information**

**Citation:** Xu, F., Linnebur, K., & Wang, D. (2014). Torrefaction of conservation reserve program biomass: A techno-economic evaluation. *Industrial Crops and Products*, 61, 382-387.

**Digital Object Identifier (DOI):** doi:10.1016/j.indcrop.2014.07.030

**Publisher's Link:** <http://www.sciencedirect.com/science/article/pii/S0926669014004634>

This item was retrieved from the K-State Research Exchange (K-REx), the institutional repository of Kansas State University. K-REx is available at <http://krex.ksu.edu>



21 Cellulosic biomass from agricultural residues has become an important energy source because its  
22 use for biofuels production does not compete with food production; however, overuse of this  
23 biomass could cause a decrease in soil quality, and agricultural crop production could then be  
24 affected if the residue is not left for soil amendment (Lal, 2009). The Conservation Reserve  
25 Program (CRP) began in 1985 as an effort to prevent soil erosion and enhance groundwater  
26 recharge from highly erodible lands. About 30 million acres of CRP land prevent 0.3 million  
27 tons of nitrogen and 50,000 tons of phosphorous annually from flowing into river or lakes  
28 (USDA, 2012). About 50 million tons of dry biomass could be harvested annually from CRP  
29 land, indicating great potential for bioenergy production (Perlack et al., 2005). A recent study  
30 suggested that CRP biomass is a potential bioenergy feedstock if appropriate management  
31 practices are applied (Lee et al., 2013). Compared with conversion of CRP land for starch-based  
32 agricultural production such as corn and soybean, direct use of the CRP land for cellulosic  
33 biomass production would avoid carbon debt according to a recent analysis (Gelfand et al., 2011).  
34 Therefore, CRP biomass, the mixed grass from the CRP land, becomes a competitive feedstock  
35 because it does not compete with food production and could minimize soil erosion. Assuming  
36 that 20% of the total amount of CRP biomass is harvested for bioenergy production and all other  
37 biomass is left for land conservation, more than 2 million tons of cellulosic ethanol (as a  
38 representative biofuel) could be produced annually, which is equal to 5% of the 2022 cellulosic  
39 biofuels objective (16 billion gallons) made by the Energy Independence and Security Act of  
40 2007 (EISA, P.L. 110-140) (Schnepf, 2011).

41 Although recent biomass-processing techniques have proven effective in biomass conversion, the  
42 production cost of developing cellulosic biofuel remains high. Biomass upgrading through  
43 torrefaction shows great potential to benefit both the supply chain and downstream processing

44 units (Batidzirai et al., 2013; Chin et al., 2013; Ciolkosz and Wallace, 2011). The torrefaction of  
45 biomass is basically a thermal process conducted in the temperature range of 200–300 °C under  
46 under anaerobic conditions atmospheric conditions (Van der Stelt et al., 2011). Biomass moisture  
47 content (MC) is reduced in the initial drying process and biomass is partially degraded. Studies  
48 have shown that torrefaction enhanced the properties of different biomass materials (Couhert et  
49 al., 2009; Ren et al., 2012). Torrefaction is being applied to bioenergy production in thermal-  
50 chemical and biochemical platforms, and the enhanced properties after torrefaction were reported  
51 to improve the efficiency of biomass gasification and conserve chemical energy (Prins et al.,  
52 2006). Energy consumption was reported to be lower for torrefied biomass than for untorrefied  
53 biomass in the production of cellulosic ethanol (Chiaramonti et al., 2011). Torrefaction also  
54 improves biomass properties by increasing hydrophobicity. Most agricultural wastes, including  
55 grass biomass, show significant hydrophilicity, which results in problems during biomass storage,  
56 transportation, and processing; for example, biomass easily absorbs moisture, which results in  
57 decreased energy density. More importantly, hydrophilic biomass needs much more water to  
58 reduce viscosity of the slurry, resulting in increased energy consumption in the subsequent  
59 separation process. In addition, moisture absorption during storage causes fungi formation that  
60 could decrease the quality of feedstock (Rentizelas et al., 2009), whereas torrefaction provided  
61 microbial-resistant biomass, which reduces storage cost (Medic et al., 2012). Thus, torrefaction  
62 offers great potential for the biomass processing chain.

63 In this paper, we report the first study of CRP biomass enhancement through torrefaction.  
64 Changes in CRP biomass were investigated through different techniques. To integrate the  
65 torrefaction unit into the biomass processing system, an economic evaluation is critical for  
66 commercial application. We conducted our technical analysis including the results of mass and

67 energy balances. Following the analysis of torrefaction unit, we analyzed how torrefaction  
68 affected related biomass processing units such as transportation, grinding, and pelletization.

## 69 **2. Experimental section**

### 70 2.1. Materials

71 The CRP biomass was harvested in 2012 from Valley Falls, Kansas, and field-dried to reduce the  
72 MC to about 20%. The biomass was then stored in plastic bag at 4 °C. All chemicals used in this  
73 study were from Sigma-Aldrich, Inc. (St. Louis, MO).

### 74 2.2. Torrefaction

75 The torrefaction experiments were conducted using a Parr 4570 pressure reactor with a Parr 4848  
76 temperature controller (Parr Instrument Co., Moline, IL). CRP biomass was cut to about 10 cm  
77 in length before loading. After biomass loading, the reactor was filled with a nitrogen flux to  
78 completely remove oxygen. Experiments tested different combinations of temperature (200, 250,  
79 and 300 °C) and time (15, 30, and 45 min). Volatile chemicals were collected with a cold trap  
80 before exhausting to the atmosphere. After treatment, the reactor was immediately cooled with  
81 water. Samples were weighed and collected for further analysis.

### 82 2.3. Compositional analysis

83 The structural polymer (cellulose, hemicellulose, and lignin) and MC of the CRP biomass were  
84 analyzed following procedures from the National Renewable Energy Laboratory (NREL) (Sluiter  
85 et al., 2004). The elemental composition was measured with CHNS/O Elemental Analyzer  
86 (PerkinElmer 2400 Series II, PerkinElmer Inc., Waltham, MA). About 3 mg of the ground  
87 sample was weighed using a PerkinElmer AD-6 Autobalance (PerkinElmer Inc., Waltham, MA),

88 and was then introduced into the combustion chamber for burning under pure oxygen  
89 atmosphere. The gases from combustion were separated in a quartz column containing copper  
90 wires and detected by a thermoconductometer. Results are reported as a percentage of initial dry  
91 weight (w/w).

#### 92 2.4. Thermogravimetric Analysis (TGA)

93 Decomposition characteristics of the biomass were analyzed by thermal gravimetric analysis  
94 (TGA) (Perkin-Elmer TGA Pyris 7, Norwalk, CT). Around 5 mg of sample was measured at a  
95 heating rate of 20 °C/min from 40 to 700 °C under a dry nitrogen flux. Both percentage weight  
96 change and derivative weight were reported.

#### 97 2.5. High heating value (HHV)

98 The HHV of the CRP biomass was determined by a calorimeter (IKA-Calorimeter C 200, IKA-  
99 Werke GmbH and Co. KG, Staufen, Germany) with a benzoic acid standard. After grinding,  
100 about 1 g of sample was pelletized then loaded into an adiabatic bomb for burning. The released  
101 energy was reported in Megajoule (MJ) per kg. The HHV was also calculated using the  
102 elemental results for comparison according to the equation (Sheng and Azevedo, 2005):

$$103 \quad HHV \text{ (MJ/Kg)} = -1.3675 + 0.3137 \times C + 0.7009 \times H + 0.0318 \times O$$

#### 104 2.6. Energy balance

105 The energy and mass flow was modeled using Aspen Plus 7.3, as shown in Figure 1. The energy  
106 balance for torrefaction unit was studied by considering the total energy input ( $E_I$ ), the total  
107 energy output ( $E_O$ ), the high heating value of biomass before and after torrefaction ( $HHV_m$  and  
108  $HHV_{m'}$ , respectively), process energy input ( $E_p$ ), and energy loss ( $E_l$ ) and using the following

109 equations. Energy analysis was conducted assuming the volatiles are combusted to supply energy  
110 to the system.

$$111 \quad EI = EO$$

$$112 \quad EI = HHV_m + E_p$$

$$113 \quad EO = HHV_{tm} + E_l$$

114 The net energy efficiency ( $e_{net}$ ) was defined here as the ratio of  $HHV_{tm}$  to  $EI$ .

$$115 \quad e_{net} = (HHV_{tm} / EI) \times 100\%$$

## 116 2.7. Economic analysis

117 Economic analysis employs spreadsheet investment analysis calculations. Equipment costs were  
118 estimated by Aspen software. Operation conditions were either from the literature or current  
119 study. Other key assumptions were discussed in Section 3.2.

120

## 121 **3. Results and discussion**

### 122 3.1. Characteristics of torrefied biomass

#### 123 3.1.1. Mass loss

124 The effects of torrefaction temperature and time on the dry mass loss of CRP biomass were  
125 investigated; results are shown in Figure 2. Previous reports showed that biomass MC  
126 significantly affected the dry mass recovery after torrefaction and almost 50% (wet base) of  
127 biomass lost (Van der Stelt et al., 2011). In this study, the mass loss was up to 35% at 300 °C  
128 because the CRP biomass has a relatively low MC (about 20%) after a field dry. As shown in  
129 Figure 2, the dry mass loss increased as processing temperature and time increased. A significant

130 jump in dry mass loss occurred when the temperature increased from 250 to 300 °C, probably  
131 because one or more biomass components was degraded at the higher temperature. Further  
132 composition analysis is necessary to better understand the increase in mass loss.

### 133 3.1.2. Polymer composition analysis

134 Since temperature significantly affects biomass loss, a detailed composition analysis including  
135 structural polymers and elements was conducted to understand how the processing temperature  
136 changed biomass structure. A previous review suggested that hemicellulose is extensively de-  
137 volatilized at high temperatures (e.g., 250–260 °C) (Van der Stelt et al., 2011), but most studies  
138 didn't provide evidence of detailed investigation of hemicellulose change in biomass torrefaction.  
139 In addition, although individual polymers/monosaccharides were used in a previous torrefaction  
140 study (Chen et al., 2011), the results might not be useful to predict compositional changes in  
141 biomass because of the complex structure of biomass. In this study, we analyzed the  
142 compositional change of three polymers, cellulose, xylan (the major polymer in hemicellulose),  
143 and lignin using the NREL methods. As shown in Table 1, the xylan content decreased  
144 significantly as the temperature increased from 200 to 300 °C, but xylan was not completely  
145 degraded even at 300 °C. About 25% of xylan remained according to weight loss measured at  
146 300 °C, probably because the other polymers in the twisted structure of the biomass protect  
147 xylan from complete degradation. Also found is the decrease of cellulose. Cellulose showed less  
148 degradation than hemicellulose at the same temperature, because cellulose contains a well-  
149 ordered crystalline structure (Xu et al., 2013). Considering the significant dry mass loss (Fig. 2),  
150 it was calculated that about half of the cellulose was degraded at 300 °C. Lignin, however, was  
151 more thermally stable in the studied temperature range. Another recent report also suggested that  
152 lignin content didn't changed significantly in the temperature range of 230–290 °C (Chen and



153 Kuo, 2011). Because the degradation of cellulose means loss of biomass heating value,  
154 torrefaction conditions should be managed appropriately.

### 155 3.1.3. TGA

156 To understand the effects of temperature on biomass in a wide temperature range, TGA was  
157 conducted to show the dynamic weight change of the CRP biomass (Fig. 3). As the temperature  
158 increased to 250 °C, biomass weight percentage decreased slowly. A light biomass torrefaction  
159 was considered at around 240 °C (Van der Stelt et al., 2011). With further increase in  
160 temperature, the weight started to decrease dramatically according to the weight derivative curve  
161 due to significant hemicellulose loss. At this stage (260–300 °C), cellulose and lignin remain the  
162 major energy components. The partial loss of cellulose, as shown in compositional analysis,  
163 could be due to the degradation of amorphous cellulose, which is more sensitive to heat reactions  
164 than crystalline cellulose. Further increasing the temperature resulted in a sharp drop in weight  
165 percentage. The maximum rate of weight decrease occurred around 350 °C because of the  
166 pyrolysis of cellulose and partial degradation of lignin (Yang et al., 2007). Lignin then became  
167 the major energy source in the biomass. It is concluded that biomass structure as well as its  
168 characteristics change depending on torrefaction conditions; therefore, a temperature control  
169 strategy could be used to produce torrefied biomass with desired characteristics.

### 170 3.1.4. Elemental composition

171 Elemental analysis was then conducted to show changes in three elemental components (C, H,  
172 and O) (Table 1). Results suggested that the weight percentages of the components did not  
173 change significantly, but both the atomic ratios of O/C and H/C decreased. The removal of MC  
174 and the de-volatilization of formed CO<sub>2</sub> could have contributed to the decreases (Tapasvi et al.,  
175 2012). A Van Krevelen diagram was then built with all experimental data to show the

176 relationships of elemental ratios (Fig. 4). Both the atomic ratios of O/C and H/C displayed a  
177 decreasing trend as the temperature increased. The chemical properties of torrefied biomass vary  
178 depending on processing conditions, but they differ from coal, which has lower ratios of both  
179 H/C and O/C (Fig. 4). The degradation of hemicellulose resulted in the loss of hydroxyl group  
180 instead of a simple loss of xylan, considering the fact that xylan,  $(C_5H_8O_4)_n$ , has an O/C ratio of  
181 0.8. Similarly, the glucan unit of cellulose,  $(C_6H_{10}O_5)_n$ , has an O/C ratio less than 1. Results  
182 suggested that the polysaccharides were converted to other polymers/molecules with higher  
183 carbon content. Further structural analysis is suggested to understand the effects of torrefaction  
184 on biomass structure.

### 185 3.1.5 Heating value and energy density

186 After torrefaction, the HHV of biomass increased with processing temperature but didn't change  
187 significantly with increased processing time (Table 2). A calculated HHV was also listed for  
188 comparison, suggesting that a rough estimation of the biomass HHV could be obtained by  
189 elemental results. Energy density increased up to 18% when processed at 300 °C for 45 minutes.  
190 The removal of hydroxyl groups increased carbon percentage as well as the percentage of C-C  
191 bonds, which is an important reason for the increased energy density.

192 Energy recovery (ER) decreased with the increasing temperature. The torrefied CRP biomass at  
193 300 °C and 45 minutes retained only about 76% of the energy in the original biomass as a result  
194 of mass loss; note that recovery was calculated on solid biomass. If the energy carried by  
195 volatiles is recycled for combustion, net energy efficiency will increase. Further economic  
196 analysis is discussed below.

## 197 **3.2. Economic potential**

### 198 3.2.1. Energy input of torrefaction

199 Before an economic evaluation of torrefaction was made, energy flow as well as mass flow was  
200 analyzed and provided as shown in Figure 1. The energy required for the torrefaction process ( $E_p$ )  
201 was estimated from the sensible heat energy that increases the biomass to certain temperatures.  
202 The efficiency of energy input was considered at 60% because of heat loss (Bergman and Kiel,  
203 2005). The energy balance for the torrefaction system was then investigated based on energy  
204 content results shown in Table 2. The net thermal efficiency of torrefaction ( $e_{net}$ ) was in the range  
205 of 80–90% because most torrefaction gas could be used through combustion in a practical  
206 application (Uslu et al., 2008).

207 Sensitivity analysis was then performed to investigate how the energy required for the  
208 torrefaction process is affected by changing variables. Figure 5 shows a sensitivity analysis of  
209 energy input with different processing temperatures and times.  $E_p$  increased significantly with  
210 increasing temperature as a result of increased sensible heat energy. The significant biomass loss  
211 at a higher temperature results in more degradation products including volatiles, which means  
212 that more energy was required to break the chemical bonds. Although most of the heat energy in  
213 volatiles could be recycled (Fig. 1), the energy reduction in the solid fraction increased with  
214 increasing volatiles. This result also explains why  $E_p$  increased as the processing time increased,  
215 because the energy loss to the environment increased during the accumulation period. A previous  
216 study suggested that biomass MC (in the range of 20 to 60%) affects energy input because the  
217 water evaporation consumes additional energy during torrefaction (Ciolkosz and Wallace, 2011),  
218 but the sensitivity analysis in this study did not include it because the MC of CRP biomass was  
219 less than 20%.

220 3.2.2. Cost estimate for torrefaction process

221 The economic analysis was conducted on the basis of total feedstock cost (\$/ton feedstock). The  
222 capital cost was evaluated using a capacity-factored estimation and according to previous  
223 torrefaction studies (Bergman et al., 2005). For the costs of installation, depreciation, and  
224 financing, the estimation was related to capital investment. This study also used a factorial  
225 method to categorize the breakdown list of production costs (Peters et al., 1968). For operation  
226 costs such as labor, maintenance, fuel gas, and utilities, the estimate was based on the capacity  
227 and the nature of the processing plant.

228 As mentioned in the Section 1, CRP biomass grows in different states and yields over 10 million  
229 tons of biomass for bioprocessing (about 1/5 of total amount) after leaving most of the biomass  
230 for land conservation. Multiple torrefaction plants are expected in different CRP sections. The  
231 cost estimation was based on a torrefaction plant with an annual capacity of 100,000 tons with an  
232 operation window of 6 months per year. The daily processing capacity for incoming feedstock is  
233 about 600 tons, and the useful life of the plant was assumed to be 20 years. The total processing  
234 costs comprise capital costs and operation costs. The direct capital cost was estimated at \$8  
235 million, include plant construction, equipment costs, and installation but excluding engineering  
236 management costs (Uslu et al., 2008). The finance costs were set to an annual interest of 8%,  
237 which was calculated as about \$1.6 per ton of feedstock. The total capital cost was calculated as  
238 \$6.6 per ton of feedstock.

239 Operation costs include energy, labor, management, maintenance, etc. Cost of feedstock was not  
240 included in the operation cost. The energy cost was calculated from the energy input of the unit  
241 process and a recent gas fuel price (\$3.8/GJ) (USEIA, 2013). Labor cost was calculated on an  
242 hourly rate of \$20 and 6 months/year, which is \$2 per ton. Considering a depreciation period of  
243 10 years, the cost of depreciation was calculated as \$5.5 per ton. (Other details are in Table 3.)

244 The total operation cost was calculated as \$9.7 per ton. Total unit costs of torrefaction are \$16.3  
245 per ton of feedstock, which is equal to about \$23 per ton of torrefied biomass. Note that the  
246 operation cost was estimated assuming that the CRP biomass contains no more than 20% MC. If  
247 the CRP biomass were not dried before torrefaction, operation and capital costs would increase.

248

### 249 3.2.3. Comparison of torrefaction with other processes

250 The torrefaction process provides not only an upgrade to biomass quality but also great economic  
251 potential for the whole biomass supply chain. Economic analysis was performed to compare  
252 three biomass processing units: Torrefaction, pelletization, and a combined unit of torrefaction  
253 and pelletization (TOP). Before biomass pelletization, an energy-consuming grinding process is  
254 necessary. The grinding energy of torrefied wood chips could be reduced to as low as 24 kW h/t  
255 (at torrefaction temperature of 300 °C), which is about 1/10 of the energy needed for the grinding  
256 of raw biomass (Phanphanich and Mani, 2011). This decrease in energy requirements occurs  
257 because torrefaction reduces biomass particle size and renders biomass more brittle (Medic et al.,  
258 2012) and because the hammer mills used in conventional pelletization can be replaced by a  
259 simple cutting mill (Arias et al., 2008). The cost savings were calculated as about \$3–10 per ton  
260 depending on the grinding scale and energy source. In addition, torrefaction could benefit the  
261 pelletization process. A previous study suggested that pelletization of torrefied biomass saved  
262 about 20% of the energy required for conventional pelletization by increasing energy efficiency  
263 (Thek and Obernberger, 2004). Economic evaluations of three biomass-processing techniques  
264 are performed and compared in Table 3. The initial capital costs for a biomass plant with an  
265 annual capacity of 100,000 tons were estimated as \$8 million, \$7 million, and \$10 million for  
266 torrefaction, pelletization, and TOP plant, respectively. The data for pelletization were based on

267 previous study (Thek and Obernberger, 2004) and were normalized to the same scale as this  
268 study for comparison. Construction and management costs were estimated on the scale of capital  
269 volume.

270 Besides saving production cost, further analysis showed that the biomass upgrade could reduce  
271 the cost of transportation. Although the bulk density of torrefied biomass does not increase  
272 significantly, the increase in energy density could decrease transportation cost based on units of  
273 energy value. A previous study suggested that the average transportation cost of agricultural  
274 biomass by truck is about  $\$1/(\text{GJ} \cdot 100\text{Km})$  (Searcy et al., 2007). Combined with pelletization,  
275 our analysis showed that the transportation cost of TOP ( $\$0.28/(\text{GJ} \cdot 100\text{Km})$ ) could decrease up  
276 to 30% compared with conventional pelletization ( $\$0.4/(\text{GJ} \cdot 100\text{Km})$ ) (Table 3). Thus, the TOP  
277 process offers benefits to biomass logistics.

#### 278 **4. Conclusions**

279 Using CRP biomass for bioenergy production has great potential and minimizes soil erosion.  
280 Biomass torrefaction upgrades biomass properties by increasing energy density, reducing MC,  
281 reducing particle size, increasing hydrophobicity, and increasing brittleness for easier grinding.  
282 The study on biomass composition, especially polymer composition, suggested that the  
283 polysaccharides in biomass were converted to other high-carbon content materials. Preserving  
284 energy content (e.g., cellulose and lignin) and polysaccharide content (e.g., cellulose and xylan)  
285 in biomass during torrefaction is suggested. The economic evaluation found that costs of the  
286 torrefaction process were about  $\$16.3$  per ton of feedstock (or  $\$23$  per ton of product). A  
287 comparison of torrefaction and pelletization showed that the combined TOP process could  
288 benefit the biomass supply chain by upgraded biomass quality and reduced processing (e.g.,  
289 grinding), storage, and transportation costs.

290 **Acknowledgments**

291 This is contribution number 14-010-J from the Kansas Agricultural Experiment Station.

292

293

References

294

295 Arias, B., Pevida, C., Feroso, J., Plaza, M., Rubiera, F., Pis, J., 2008. Influence of torrefaction  
296 on the grindability and reactivity of woody biomass. *Fuel Processing Technology* 89, 169-175.

297 [Batidzirai, B., Mignot, A., Schakel, W., Junginger, H., Faaij, A., 2013. Biomass torrefaction  
298 technology: Techno-economic status and future prospects. \*Energy\* 62, 196-214.](#)

299 Bergman, P., 2005. Combined torrefaction and pelletisation. Energy Research Centre of the  
300 Netherlands, ECN-C-05-073.

301 Bergman, P., Boersma, A., Zwart, R., Kiel, J., 2005. Torrefaction for biomass co-firing in  
302 existing coal-fired power stations. Energy Research Centre of the Netherlands, ECN-C-05-013.

303 [Bergman, P., Kiel, J., 2005. Torrefaction for biomass upgrading, 14th European Biomass  
304 Conference & Exhibition, Paris, France.](#)

305 Chen, W.-H., Cheng, W.-Y., Lu, K.-M., Huang, Y.-P., 2011. An evaluation on improvement of  
306 pulverized biomass property for solid fuel through torrefaction. *Applied Energy* 88, 3636-3644.

307 Chen, W.-H., Kuo, P.-C., 2011. Torrefaction and co-torrefaction characterization of  
308 hemicellulose, cellulose and lignin as well as torrefaction of some basic constituents in biomass.  
309 *Energy* 36, 803-811.

310 Chiamonti, D., Rizzo, A.M., Prussi, M., Tedeschi, S., Zimbardi, F., Braccio, G., Viola, E.,  
311 Pardelli, P.T., 2011. 2nd generation lignocellulosic bioethanol: is torrefaction a possible  
312 approach to biomass pretreatment? *Biomass Conversion and Biorefinery* 1, 9-15.

313 [Chin, K., H'ng, P., Go, W., Wong, W., Lim, T., Maminski, M., Paridah, M., Luqman, A., 2013.  
314 Optimization of torrefaction conditions for high energy density solid biofuel from oil palm  
315 biomass and fast growing species available in Malaysia. \*Industrial Crops and Products\* 49, 768-  
316 774.](#)

317 Ciolkosz, D., Wallace, R., 2011. A review of torrefaction for bioenergy feedstock production.  
318 *Biofuels, Bioproducts and Biorefining* 5, 317-329.

319 Couhert, C., Salvador, S., Commandre, J., 2009. Impact of torrefaction on syngas production  
320 from wood. *Fuel* 88, 2286-2290.

321 Gelfand, I., Zenone, T., Jasrotia, P., Chen, J., Hamilton, S.K., Robertson, G.P., 2011. Carbon  
322 debt of Conservation Reserve Program (CRP) grasslands converted to bioenergy production.  
323 *Proceedings of the National Academy of Sciences* 108, 13864-13869.

324 Lal, R., 2009. Soil quality impacts of residue removal for bioethanol production. *Soil and tillage  
325 research* 102, 233-241.

326 Lee, D.K., Aberle, E., Chen, C., Egenolf, J., Harmony, K., Kakani, G., Kallenbach, R.L., Castro,  
327 J.C., 2013. Nitrogen and harvest management of Conservation Reserve Program (CRP) grassland  
328 for sustainable biomass feedstock production. *GCB Bioenergy* 5, 6-15.

329 Medic, D., Darr, M., Shah, A., Rahn, S., 2012. Effect of Torrefaction on Water Vapor  
330 Adsorption Properties and Resistance to Microbial Degradation of Corn Stover. *Energy & Fuels*  
331 26, 2386-2393.

332 Perlack, R.D., Wright, L.L., Turhollow, A.F., Graham, R.L., Stokes, B.J., Erbach, D.C., 2005.  
333 Biomass as feedstock for a bioenergy and bioproducts industry: the technical feasibility of a  
334 billion-ton annual supply, in: report, U.a.D. (Ed.). Oak ridge national laboratory.

335 Peters, M.S., Timmerhaus, K.D., West, R.E., Timmerhaus, K., West, R., 1968. Plant design and  
336 economics for chemical engineers. McGraw-Hill New York.

337 Phanphanich, M., Mani, S., 2011. Impact of torrefaction on the grindability and fuel  
338 characteristics of forest biomass. *Bioresource technology* 102, 1246-1253.

339 Prins, M.J., Ptasiński, K.J., Janssen, F.J., 2006. More efficient biomass gasification via  
340 torrefaction. *Energy* 31, 3458-3470.

341 Ren, S., Lei, H., Wang, L., Bu, Q., Chen, S., Wu, J., Julson, J., Ruan, R., 2012. The effects of  
342 torrefaction on compositions of bio-oil and syngas from biomass pyrolysis by microwave heating.  
343 *Bioresource technology*.

344 Rentizelas, A.A., Tolis, A.J., Tatsiopoulou, I.P., 2009. Logistics issues of biomass: The storage  
345 problem and the multi-biomass supply chain. *Renewable and Sustainable Energy Reviews* 13,  
346 887-894.

347 Schnepf, R., 2011. Renewable fuel standard (RFS): overview and issues. DIANE Publishing.

348 Searcy, E., Flynn, P., Ghafoori, E., Kumar, A., 2007. The relative cost of biomass energy  
349 transport. *Applied biochemistry and biotechnology* 137, 639-652.

350 Sheng, C., Azevedo, J., 2005. Estimating the higher heating value of biomass fuels from basic  
351 analysis data. *Biomass and Bioenergy* 28, 499-507.

352 Sluiter, A., Hames, B., Ruiz, R., Scarlata, C., Sluiter, J., Templeton, D., Crocker, D., 2004.  
353 Determination of structural carbohydrates and lignin in biomass. NREL, Golden, CO.

354 Tapasvi, D., Khalil, R., Skreiberg, Ø., Tran, K.-Q., Grønli, M., 2012. Torrefaction of Norwegian  
355 Birch and Spruce: An Experimental Study Using Macro-TGA. *Energy & Fuels* 26, 5232-5240.

356 Thek, G., Obernberger, I., 2004. Wood pellet production costs under Austrian and in comparison  
357 to Swedish framework conditions. *Biomass and Bioenergy* 27, 671-693.

358 USDA, 2012. Agriculture Secretary Vilsack Announces New Conservation Reserve Program  
359 Initiative to Restore Grasslands, Wetlands and Wildlife.

360 USEIA, 2013. Natural Gas Weekly Update.

361 Uslu, A., Faaij, A.P., Bergman, P., 2008. Pre-treatment technologies, and their effect on  
362 international bioenergy supply chain logistics. Techno-economic evaluation of torrefaction, fast  
363 pyrolysis and pelletisation. *Energy* 33, 1206-1223.



- 364 Van der Stelt, M., Gerhauser, H., Kiel, J., Ptasinski, K., 2011. Biomass upgrading by torrefaction  
365 for the production of biofuels: A review. *Biomass and Bioenergy* 35, 3748-3762.
- 366 Xu, F., Shi, Y.-C., Wang, D., 2013. X-ray scattering studies of lignocellulosic biomass: A review.  
367 *Carbohydrate Polymers* 94, 904-917.
- 368 Yang, H., Yan, R., Chen, H., Lee, D.H., Zheng, C., 2007. Characteristics of hemicellulose,  
369 cellulose and lignin pyrolysis. *Fuel* 86, 1781-1788.
- 370
- 371

372 Table 1. Compositional and elemental analysis of CRP biomass (%)<sup>a</sup>

Conditions	Polymers				Elements				Ratio	
	Cellulose	Xylan	Lignin	Arabinan	C	H	N	O	O/C	H/C
200 °C	27.62	15.66	14.08	4.39	48.3	5.6	1.8	42.8	0.66	1.39
250 °C	26.95	12.45	15.84	3.54	49.8	5.4	2.1	41.1	0.62	1.30
300 °C	22.49	6.63	19.25	2.24	52.9	5.1	2.1	38.6	0.55	1.16
Control	30.18	17.43	13.01	5.69	46.6	5.4	1.7	45.0	0.72	1.39

373 <sup>a</sup> Data shown are the average of replicates. Processing temperature is 30 minutes.

374

375 Table 2. Heating value and energy density changes of CRP biomass

Temperature, °C Time, min	Control	200			250			300		
		15	30	45	15	30	45	15	30	45
HHV (MJ/Kg) <sup>a</sup>	18.36	18.80	18.87	18.89	19.49	19.41	19.42	20.41	21.13	21.68
HHV <sub>c</sub> (MJ/Kg) <sup>b</sup>	18.43	18.92	19.09	19.31	19.43	19.39	19.30	19.72	20.01	21.00
ED increase (%) <sup>c</sup>	0	2.4	2.8	2.9	6.2	5.7	5.8	11.2	15.1	18.1
ER <sup>d</sup> (%)	100	92.9	92.0	90.6	89.7	87.6	87.7	76.8	78.4	76.0

376 <sup>a</sup>HHV: Higher heating value determined by a calorimeter.

377 <sup>b</sup>HHV<sub>c</sub>: Higher heating value calculated based on elemental results.

378 <sup>c</sup>ED: Energy density, calculated as the energy value on unit volume (MJ/m<sup>3</sup>).

379 <sup>d</sup>ER: Energy recovery, calculated as energy in solid fraction.

380

381 Table 3. Total cost comparison of three processing techniques<sup>a</sup>

Items	Torrefaction	Pelletization	TOP <sup>b</sup>
<b>A. Capital costs</b>			
Capital investment, \$ (in millions)	8	7	10
Annual capacity, tons/year	100,000	100,000	100,000
Financing (8%), \$/ton	1.6	1.4	2
C&M, \$/ton <sup>c</sup>	1	0.8	1.2
Subtotal, \$/ton	6.6	5.7	8.2
<b>B. Operation costs</b>			
Fuel gas cost, \$/ton	0.76	1.37	1.63
Utility, \$/ton	0.2	0.3	0.3
Labor, \$/ton	2.00	2.69	2.80
Maintenance, \$/ton	0.20	0.20	0.24
Depreciation, \$/ton	5.5	5.0	6.8
Plant overhead, \$/ton	1.0	0.8	1.5
Subtotal, \$/ton	9.66	10.36	13.27
<b>C. Transportation</b>			
Energy density, GJ/ton	21	16	21
Cost in 100 Km, \$/GJ	1	0.38	0.28

382 <sup>a</sup> The analysis was based on raw feedstock (ton). References: (Bergman, 2005; USEIA, 2013; Van der Stelt et al.,  
 383 2011).

384 <sup>b</sup> TOP: Combined unit of torrefaction and pelletization.

385 <sup>c</sup>C&M: Construction and management.

386

387

388 Figure captions.

389 Figure 1. Energy and mass flow of biomass torrefaction (Processing condition: 250 °C; TOR:  
390 Torrefaction, HE: Heat exchangers, COM: Combustion, EI: Energy input, EL: Energy loss, HER:  
391 Heat recycle.)

392 Figure 2. Dry mass loss of CRP biomass during torrefaction.

393 Figure 3. Thermal gravimetric and derivative gravimetric analysis of CRP biomass.

394 Figure 4. Van Krevelen diagram of CRP biomass (○: Control biomass; ◆: Torrefied biomass).

395 Figure 5. Process energy input ( $E_p$ ) for torrefaction unit.

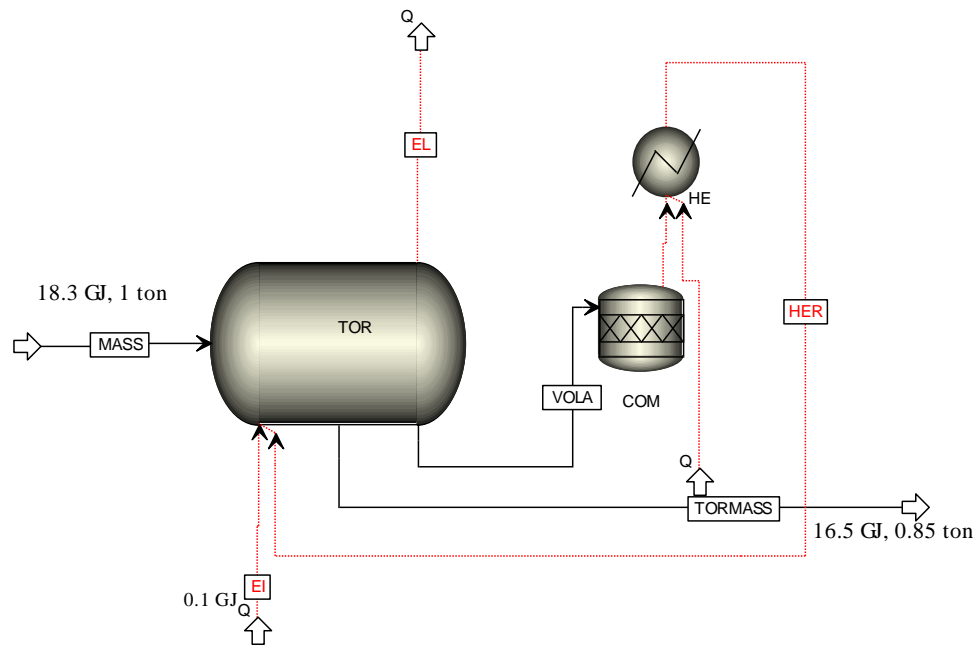


Figure 1. Energy and mass flow of biomass torrefaction (Processing condition: 250 °C; TOR: Torrefaction, HE: Heat exchangers, COM: Combustion, EI: Energy input, EL: Energy loss, HER: Heat recycle.)

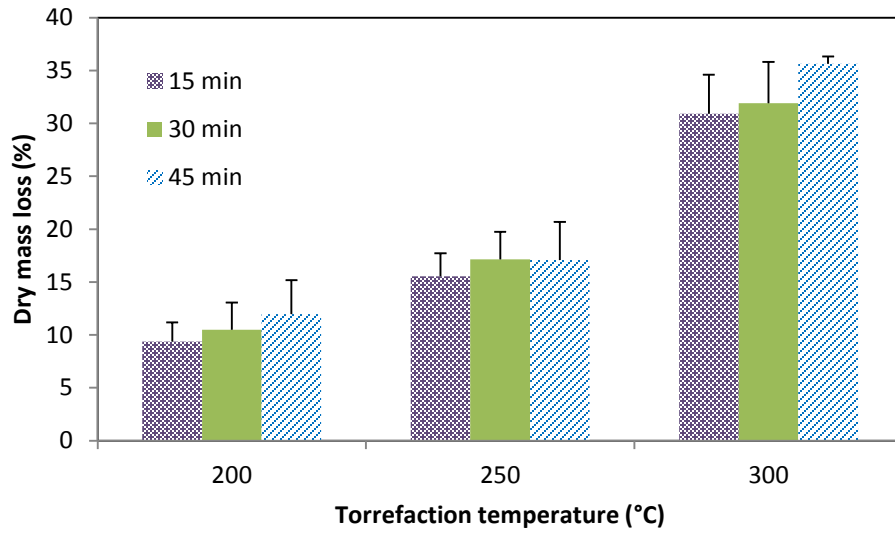


Figure 2. Dry mass loss of CRP biomass during torrefaction.

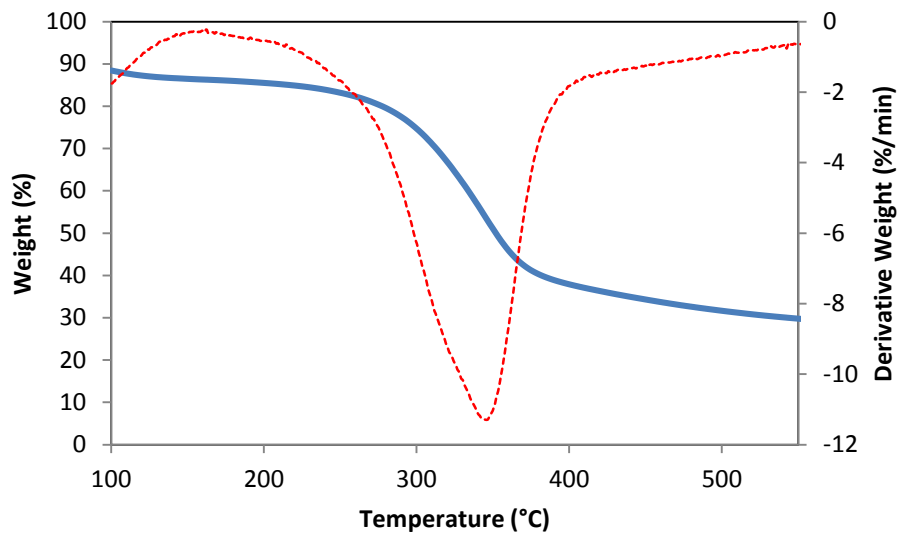


Figure 3. Thermal gravimetric and derivative gravimetric analysis of CRP biomass.



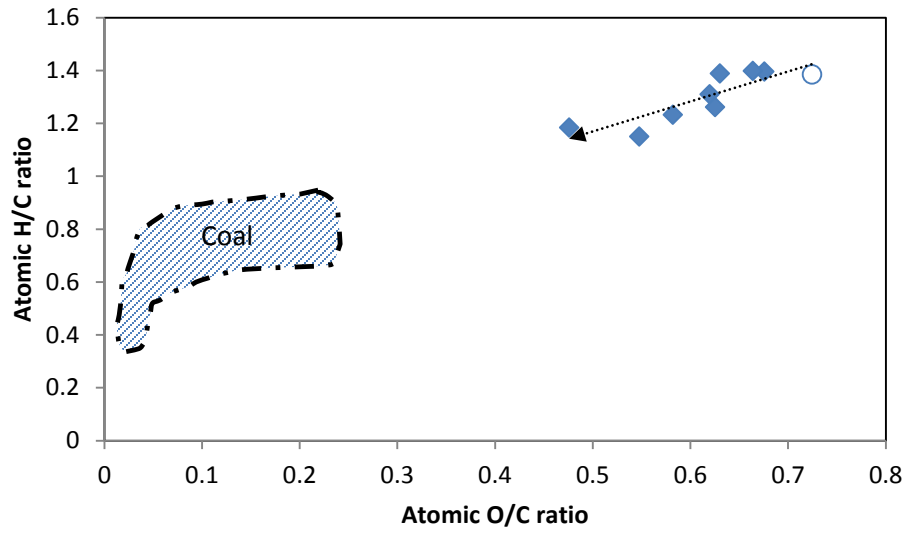


Figure 4. Van Krevelen diagram of CRP biomass (○: Control biomass; ◆: Torrefied biomass).

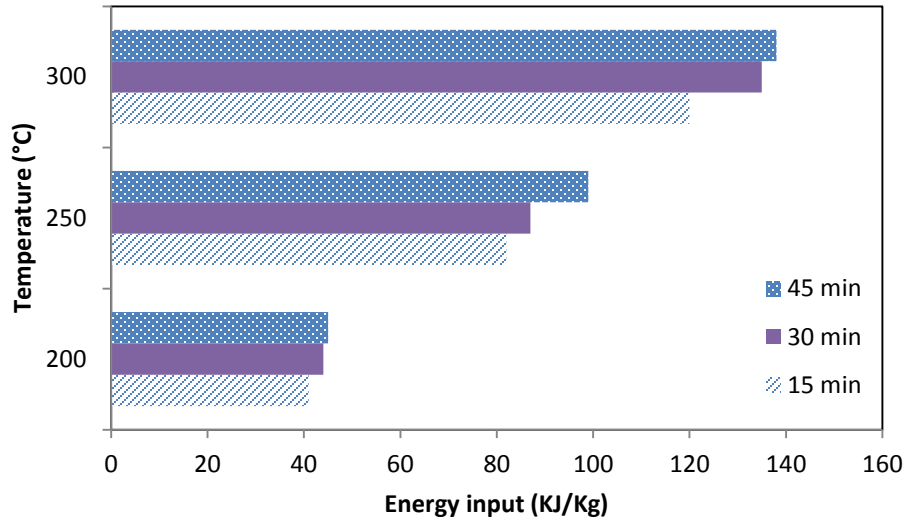


Figure 5. Process energy input ( $E_p$ ) for torrefaction unit.